Development of a homogeneous time-resolved FRET (HTRF) assay for the quantification of Shiga toxin 2 produced by *E. coli*

Keiji Nakamura [1], **Chikashi Tokuda** [2], **Hideyuki Arimitsu** [3], **Yoshiki Etoh** [4], **Mitsuhiro Hamasaki** [4], **Yuichiro Deguchi** [5], **Itsuki Taniguchi** [1], **Yasuhiro Gotoh** [1], **Yoshitoshi Ogura** [6], **Tetsuya Hayashi** [Corresp. 1]

[1] Department of Bacteriology, Graduate School of Medical Sciences, Kyushu University, Fukuoka, Japan

[2] Cisbio K.K., Chiba, Japan

[3] School of Human Science and Environment, University of Hyogo, Himeji, Japan

[4] Fukuoka Institute for Public Health and Environmental Sciences, Dazaifu, Japan

[5] Production Medicine Center, Agricultural Mutual Aid Association in Miyazaki Prefecture, Koyugun-Shintomicho, Japan

[6] Division of Microbiology, Department of Infectious Medicine, Kurume University School of Medicine, Kurume, Japan

Corresponding Author: Tetsuya Hayashi
Email address: thayash@bact.med.kyushu-u.ac.jp

Shiga toxin-producing *Escherichia coli* (STEC) is a major intestinal pathogen and causes serious gastrointestinal illness, which includes diarrhea, hemorrhagic colitis, and life-threatening hemolytic uremic syndrome. The major virulence factors of STEC are Shiga toxins (Stx1 and Stx2), which belong to the AB-type toxin family. Among several subtypes of Stx1 and Stx2, the production of Stx2a is thought to be a risk factor for severe STEC infections, but Stx2a production levels vary markedly between STEC strains, even strains with the same serotype. Therefore, quantitative analyses of Stx2 production by STEC strains are important to understand the virulence potential of specific lineages or sublineages. In this study, we developed a novel Stx2 quantification method by utilizing homogeneous time-resolved fluorescence resonance energy transfer (HTRF) technology. To determine suitable "sandwich" assay conditions, we tested 6 combinations of fluorescence-labeled monoclonal antibodies (mAbs) specific to Stx2 and compared the HTRF signal intensities obtained at various incubation times. Through this analysis, we selected the most suitable mAb pair, one recognizing the A subunit and the other recognizing the B subunit, thus together detecting Stx holotoxins. The optimal incubation time was also determined (18 hrs). Then, we optimized the concentrations of the two mAbs based on the range for linearity. The established HTRF assay detected 0.5 ng/ml of the highly purified recombinant Stx2a and Stx2e proteins and the working range was 1-64 ng/ml for both Stx2a and Stx2e. Through the quantification analysis of Stx proteins in STEC cell lysates, we confirmed that other Stx2 subtypes (Stx2b, Stx2c, Stx2d, and Stx2g) can also be quantified at a certain level of accuracy, while this assay system does not detect

Stx2f, which is highly divergent in sequence from other Stx2 subtypes, and Stx1. As the HTRF protocol we established is simple, this assay system should prove useful for the quantitative analysis of Stx2 production levels of a large number of STEC strains.

Development of a homogeneous time-resolved FRET (HTRF) assay for the quantification of Shiga toxin 2 produced by *E. coli*.

6   Keiji Nakamura[1], Chikashi Tokuda[2], Hideyuki Arimitsu[3], Yoshiki Etoh[4], Mitsuhiro Hamasaki[4],

7   Yuichiro Deguchi[5], Itsuki Taniguchi[1], Yasuhiro Gotoh[1], Yoshitoshi Ogura[6], Tetsuya Hayashi[1]

9   [1] Department of Bacteriology, Graduate School of Medical Sciences, Kyushu University, Fukuoka,

10   Fukuoka, Japan

11   [2] Cisbio K.K., Chiba, Chiba, Japan

12   [3] School of Human Science and Environment, University of Hyogo, Himeji, Hyogo, Japan

13   [4] Fukuoka Institute for Public Health and Environmental Sciences, Dazaifu, Fukuoka, Japan

14   [5] Production Medicine Center, Agricultural Mutual Aid Association in Miyazaki Prefecture,

15   Koyugun-Shintomicho, Miyazaki, Japan

16   [6] Division of Microbiology, Department of Infectious Medicine, Kurume University School of

17   Medicine, Kurume, Fukuoka, Japan

19   Corresponding author:

20   Tetsuya Hayashi

21   3-1-1 Maidashi, Higashi-ku, Fukuoka, Fukuoka, 812-8582, Japan

22   Email address: thayash@bact.med.kyushu-u.ac.jp

24 **Abstract**

25   Shiga toxin-producing *Escherichia coli* (STEC) is a major intestinal pathogen and causes

26 serious gastrointestinal illness, which includes diarrhea, hemorrhagic colitis, and life-threatening

27 hemolytic uremic syndrome. The major virulence factors of STEC are Shiga toxins (Stx1 and

28 Stx2), which belong to the AB-type toxin family. Among several subtypes of Stx1 and Stx2, the

29 production of Stx2a is thought to be a risk factor for severe STEC infections, but Stx2a production

30 levels vary markedly between STEC strains, even strains with the same serotype. Therefore,

31 quantitative analyses of Stx2 production by STEC strains are important to understand the virulence

32 potential of specific lineages or sublineages. In this study, we developed a novel Stx2

33 quantification method by utilizing homogeneous time-resolved fluorescence resonance energy

34 transfer (HTRF) technology. To determine suitable "sandwich" assay conditions, we tested 6

35 combinations of fluorescence-labeled monoclonal antibodies (mAbs) specific to Stx2 and

36 compared the HTRF signal intensities obtained at various incubation times. Through this analysis,

37 we selected the most suitable mAb pair, one recognizing the A subunit and the other recognizing

38 the B subunit, thus together detecting Stx holotoxins. The optimal incubation time was also

39 determined (18 hrs). Then, we optimized the concentrations of the two mAbs based on the range

40 for linearity. The established HTRF assay detected 0.5 ng/ml of the highly purified recombinant

41 Stx2a and Stx2e proteins and the working range was 1-64 ng/ml for both Stx2a and Stx2e. Through

42 the quantification analysis of Stx proteins in STEC cell lysates, we confirmed that other Stx2

43 subtypes (Stx2b, Stx2c, Stx2d, and Stx2g) can also be quantified at a certain level of accuracy,

44 while this assay system does not detect Stx2f, which is highly divergent in sequence from other

45 Stx2 subtypes, and Stx1. As the HTRF protocol we established is simple, this assay system should

46 prove useful for the quantitative analysis of Stx2 production levels of a large number of STEC

47 strains.

48

Introduction

49

50   Shiga toxin-producing *Escherichia coli* (STEC) causes diarrhea and hemorrhagic colitis

51   with life-threatening complications, such as hemolytic uremic syndrome (HUS). Many serogroups

52   of STEC, such as O157, O26, O111, O103, O121, and O145, cause outbreaks and sporadic cases

53   worldwide (Centers for Disease Control and Prevention, 2018; European Food Safety Authority

54   and European Centre for Disease Prevention and Control, 2019; National Institute of Infectious

55   Diseases, 2018; Smith et al., 2019). While STEC possesses a broad range of virulence factors,

56   Shiga toxin (Stx, previously called Verotoxin) is the key virulence factor belonging to the AB-

57   type toxin family. Stxs are classified into two immunologically distinct types, Stx1 and Stx2, and

58   both types include several subtypes (Stx1a, Stx1c, and Stx1d; Stx2a, Stx2b, Stx2c, Stx2d, Stx2e,

59   Stx2f, and Stx2g) (Scheutz et al., 2012). Among these subtypes, Stx1 subtypes exhibit high amino

60   acid sequence similarity (>95% identity). In contrast, Stx2 subtypes exhibit a notable degree of

61   intragroup diversity. In particular, Stx2f is highly divergent from other Stx2 subtypes (70.9%-

62   77.0% amino acid sequence identities; Fig. S1).

63   Several biological and epidemiological studies have revealed that Stx2a production is

64   associated with more severe diseases and a higher risk of HUS (Bielaszewska et al., 2013; Dallman

65   et al., 2015; Fuller et al., 2011). In addition, it has been suggested that the Stx2a production level

66   may be linked to the high virulence potential of a specific lineage of STEC O157 (Ogura et al.,

67   2015). It has also been reported that Stx2a production levels vary markedly between STEC strains,

68   even between strains with the same serotype (i.e., STEC O157, O26, and O145) (Carter et al.,

69   2020; Ishijima et al., 2017; Ogura et al., 2018). Therefore, quantitative analyses of the Stx2

70   production level are important to understand the virulence potentials of specific lineages or

71   sublineages. Several immunological or molecular genetic methods for the detection of Stx proteins

72   or *stx* genes in STEC isolates have been developed (Parsons et al., 2016). However, there are only

73   a few reports that described methods to quantify Stx (Yamasaki et al., 2015; Quiñones et al., 2009).

74   Among these methods, sandwich ELISA-based methods exhibit high sensitivity and a broad

75   dynamic range (He et al., 2018; Yamazaki et al., 2013) but require multiple steps to obtain final

76   data; thus, they are sometimes difficult to use for the analysis of a large number of samples. There

77   are also potential risks of technical errors due to complicated protocols. Now in Japan, the ELISA

78   kits for Stx quantification, such as RIDASCREEN Verotoxin (R-Biopharm AG, Darmstadt,

79   Germany), are not commercially available, and thus a kit based on the reversed passive latex

80   agglutination (RPLA)-based assay (VTEC-RPLA) is used for the quantitative analysis of Stx. As

81   the protocol of this assay is simpler than ELISA, this assay has been widely used (Beutin et al.,

82   1996; Karmali et al., 1999; Chart et al., 2001; Ogura et al., 2015; Rahman et al., 2018). However,

83   it is a 2-fold dilution endpoint assay (thus semiquantitative assay) and endpoints are determined

84   based on the occurrence of agglutination subjectively by users. Therefore, it is sometimes difficult

85   to precisely determine toxin concentrations with high reproducibility between laboratories and

86   even in a laboratory. In this study, we developed a novel quantification method of Stx2 by utilizing

87   homogeneous time-resolved fluorescence resonance energy transfer (HTRF) technology (Degorce

88   et al., 2009) to quantitatively analyze the Stx2 production levels of isolated STEC strains. This

89   technology was already applied to the detection of other bacterial toxins, such as the protective

90   antigen of *Bacillus anthracis* (Cohen et al., 2014). A fluorescence resonance energy transfer

91   (FRET)-based Stx2 detection system (named AlphaLISA assay) has also been developed

92   (Armstrong et al., 2018). The method we developed is simple, requiring only mixing samples with

93   labeled antibodies and incubating them for a certain time, and the high reproducibility with a wide

94   calibration range of the method was also confirmed.

95

96   **Methods**

97   **Stx2 toxins and antibodies**

98   We used two types of Stx2a preparations as standards. One was a commercially available

99   lyophilized Stx2a preparation (Verotoxin 2; Denka Seiken, Tokyo, Japan) that was used for

100   optimizing assay conditions. The other was a highly purified recombinant Stx2a preparation,

101   which we used to evaluate the established assay. This recombinant Stx2a was expressed as a

102   holotoxin and purified as previously described (Arimitsu et al., 2016). In addition, we used a

103   commercially available Stx1 preparation (Verotoxin-1; Nacalai Tesque, Kyoto, Japan), a highly

104   purified recombinant Stx2e protein that was prepared as previously described (Arimitsu et al.,

105   2013a), and a commercially available recombinant Stx2f preparation (Abraxis, CA, USA). The

106   recombinant Stx2f protein contains an amino acid substitution at the active site in the A subunit

107   (glutamic acid at 167) and is thus enzymatically inactive.

108   For developing an HTRF assay, we used three monoclonal antibodies (mAbs):

109   MBS313194 (anti-Stx1/Stx2 B-subunit, MyBioSource), LS-C132889 (anti-Stx2 B-subunit,

110   Lifespan Biosciences), and 20273-04 (anti-Stx2 A-subunit, Nacalai Tesque). These mAbs were

111 fluorescently labeled using the Europium Cryptate labeling kit or the d2 labeling kit (both from

112 Cisbio/PerkinElmer). Donor and acceptor antibodies were labeled with europium (Eu) cryptate

113 and d2, respectively.

114

115 **Bacterial strains and preparation of cell lysates**

116 The STEC strains used in this study are listed in Table 1. They were isolated from humans

117 or animals in Japan and contained the *stx2* gene alone or along with the *stx1* gene. Except for the

118 five strains newly sequenced in this study (strains 07E033, 10E094, 11E007, EC-PM083, and EC-

119 PM098), the *stx* subtypes in all STEC strains were determined previously (references are available

120 in Table 1). We included an *stx*-negative *E. coli* strain (MG1655; Accession No. U00096) in the

121 strain set. Bacterial cells were cultured at 37°C with shaking in lysogeny broth (LB) medium. To

122 prepare cell lysates, STEC overnight cultures were inoculated in 2 mL of LB broth at a cell

123 concentration of 0.1 OD_{600} and grown to mid-log phase. Then, mitomycin C (MMC; Kyowa Kirin)

124 was added to the cultures (0.5 µg/ml at the final concentration). After a 6-hr incubation with MMC,

125 cultures were subjected to four 75-sec periods of sonication with a Bioruptor (Cosmo Bio) to

126 disrupt the STEC cells in cultures. The sonicated samples were centrifuged at 7,700 x g for 10 min,

127 and the supernatants were used as Stx2-containing cell lysates. Cell lysates without MMC-

128 treatment were also prepared similarly but without the addition of MMC.

129

130 **Optimization of the HTRF assay system**

131 For optimizing assay conditions (the combination of mAbs, incubation time, and

132 concentrations of fluorescence-labeled mAbs), the aforementioned lyophilized Verotoxin 2 and

133 three mAbs were used. The toxin in one vial was dissolved in 0.25 ml of phosphate buffered saline

134 containing 0.2% BSA and a preservative (0.1% NaN_3 or 0.05% ProClin300) and serially diluted

135 with the same buffer. Diluted toxin preparation (10 µl per reaction) was mixed with serially diluted

136 Eu- and d2-labeled mAbs (5 µl each per reaction; diluted with HTRF detection buffer (Cisbio)) in

137 all possible combinations, and the mixtures were incubated at room temperature. After a 0.5-18-

138 hr incubation, the emissions at 665 nm and 620 nm were measured by a PHERAstar FS microplate

139 reader (BMG LABTECH). Delta F values (%) of each reaction were calculated for interassay

140 comparison following the procedure described on the CisBio website (URL,

141 https://www.cisbio.jp/content/signal-treatment-and-analysis/).

142

Determination of Stx2 concentrations by the optimized HTRF assay

143

Diluted recombinant Stx2a preparation (used as a standard) or cell lysates were mixed

144

with the d2-labeled anti-Stx2 A-subunit mAb (20273-04, 0.8 µg/ml at the final concentration) and

145

the Eu-labeled anti-Stx2 B-subunit mAb (LS-C132889, 0.5 µg/ml at the final concentration). After

146

incubation for 18-24 hrs at room temperature, emissions were measured at 665 nm and 620 nm by

147

an Infinite 200 PRO (TECAN), and the ratio and delta ratio (DR) were calculated as follows:

148

Ratio = (665 nm counts/620 nm counts) x 100

149

DR = average Ratio $_{(Sample)}$ − average Ratio $_{(Diluent\ background)}$

150

Average ratios were obtained by two measurements using independently prepared Stx2 samples.

151

Based on the standard values prepared using Stx2a, curve fitting for each assay was performed

152

with a weighted four parameter logistic (4PL) model using Prism 8 software (GraphPad Software),

153

and Stx2 concentrations in cell lysates were calculated with this curve-fit model using the same

154

software.

155

156

RPLA assay

157

Stx2 concentrations in each STEC cell lysate were also semiquantitatively evaluated by

158

the RPLA assay using the VTEC-RPLA kit (Denka Seiken) according to the manufacturer's

159

instructions. This kit detects a wide range of Stx2 subtypes (including Stx2f) by capturing Stx2

160

proteins by latex beads coated with rabbit anti-Stx2 polyclonal antibody (pAb), and relative

161

concentrations are expressed as titers (the highest dilution that generates agglutination). In this

162

study, Stx2 concentrations measured by this kit were expressed as units/ml (one unit/ml is the

163

lowest concentration that generates agglutination). The detection limit of the kit was approximately

164

1 ng/ml when Stx2a was used; thus, one unit/ml corresponded to 1 ng/ml.

165

166

Genome sequencing of STEC strains

167

Genomic DNA of five STEC strains, 11E007 (*stx2b*-positive), 10E094 (*stx2d*-positive),

168

07E033 (*stx2f*-positive), EC-PM083 and EC-PM098 (*stx2e*-positive), was purified using a DNeasy

169

Blood and Tissue Kit (Qiagen). DNA libraries of the three STEC strains (*stx2b*-, *stx2d*-, and *stx2f*-

170

positive strains) and the two *stx2e*-positive strains were prepared using the QIAseq FX DNA

171

Library Kit (Qiagen) and NEBNext Ultra II FS DNA Library Prep Kit for Illumina (New England

172

173   Biolabs), respectively. Illumina sequencing and sequence assembly were performed as previously

174   described (Nakamura et al., 2020). The serotypes of all sequenced strains were determined by

175   SerotypeFinder 2.0 (https://cge.cbs.dtu.dk/services/SerotypeFinder/) (Joensen et al., 2015).

176   Subtyping of *stx* genes was performed by BLASTN search (>98.5% identity with >99% coverage)

177   with the reference sequences described previously (Scheutz et al., 2012). The draft genome

178   sequences of these five strains have been deposited in DDBJ/EMBL/GenBank under BioProject

179   accession numbers starting from PRJDB8147. All accession numbers of *stx2*-encoding sequences

180   in these strains are listed in Table 1.

181

182   **Results and Discussion**

183   **Establishment of an HTRF assay system for quantification of Stx2**

184   To detect Stx2, we employed a "sandwich" assay in which HTRF signals are generated

185   through energy transfer from donor to acceptor that are labeled on the antibodies. Three

186   commercially available mAbs were used as donors or acceptors in this study, and donors and

187   acceptors were labeled with Eu cryptate and d2, respectively. We first compared the HTRF signal

188   intensities in all combinations of mAbs (6 combinations) at various incubation times (0.5-18 hrs)

189   to determine the best pair for the sandwich assay (Fig. 1a). Three pairs (Donor/Acceptor: 20273-

190   04/LS-C132889, 20273-04/MBS313194 and MBS313194/LS-C132889) generated no or weak

191   signals. Among the remaining three pairs, the signals of the LS-C132889/20273-04 pair were the

192   highest at 18 hrs at each concentration of Stx2. In addition, this pair detected only holotoxin

193   because LS-C132889 recognizes the A subunit and 20273-04 recognizes the B subunit. Therefore,

194   we concluded that 18 hrs of incubation with Eu-labeled LS-C132889 and d2-labeled 20273-04

195   mAbs was the most suitable assay condition. It should be noted that although we employed 18-hrs

196   incubation in this study as the strongest signals were obtained, it seems possible to shorten

197   incubation time if necessary although the working range may be changed.

198   We next optimized the antibody concentrations. Under a fixed concentration of d2-labeled

199   mAb (1.0 µg/ml), the range for linearity in HTRF assays was evaluated using twofold serially

200   diluted Eu-labeled mAb by visual inspection of a plot of signals (Fig. 1b). The widest linear range

201   was observed when 0.5 µg/ml Eu-labeled mAb was used. Therefore, using this concentration of

202   Eu-labeled mAb, we performed a similar analysis to determine the optimal concentration of d2-

203   labeled mAb. Based on the results of this analysis, we decided to use 0.8 µg/ml d2-labeled mAb

204   for the assay.

205

Evaluation of the dynamic range and specificity of the HTRF assay using purified Stx
preparations (Stx2a, Stx2e, Stx2f, and Stx1a)

208   Next, we evaluated the dynamic range and specificity of the established HTRF assay
209   using four purified Stx preparations. Note that among the four preparations, the Stx2a and Stx2e
210   preparations were highly purified to homogeneity (Arimitsu, et al. 2013a; Arimitsu, et al. 2013b).
211   **Stx2a:** The HTRF assay detected 0.5 ng/ml Stx2a (Table S1), and the signal intensity reached a
212   plateau at 128 ng/ml (Fig. 2). Although a calibration curve could be drawn using the signals
213   ranging between the lower and upper limits (0.5-128 ng/ml) (Fig. S2), signals around the lower
214   limit were very weak (DR: 0.6-0.8), and the deviation of signals at 128 ng/ml was relatively larger
215   than those at other concentrations (DR: 76.1-91.5; SD = 7.8) (Table S1). By narrowing the range
216   of Stx2 (1-64 ng/ml), more reproducible signal intensity and improved linearity were achieved
217   (Table S1 and Fig. 2). Therefore, the working range was determined to be between 1 and 64 ng/ml.
218   **Stx2e:** In our HTRF assay, the detection limit of Stx2e was identical to that of Stx2a, and the
219   working range was also similar to that of Stx2a (Fig 2, Fig. S2, and Table S2). Thus, our HTRF
220   assay can quantify Stx2e with a dynamic range and sensitivity similar to those of Stx2a.
221   **Stx2f and Stx1a:** We further examined the applicability of the HTRF assay for Stx2f and Stx1a,
222   the former of which is highly divergent in amino acid sequence from other Stx2 subtypes (Fig.
223   S1). Stx2f signals were not detected even at a high concentration (1.28 μg/ml) (Table S2).
224   Furthermore, Stx2f in the cell lysate of strain 07E033, a Stx2f-producing strain, was not detected
225   by the HTRF assay, although the presence of Stx2f in the lysate was confirmed by the VTEC-
226   RPLA assay (Table 1). This result is consistent with a previous report that the antigenicity of the
227   A subunit of Stx2f is different from that of other Stx2 subtypes (Skinner et al., 2013) and suggests
228   that the mAb against the A subunit (LS-C132889) used in our HTRF assay is unable to capture
229   Stx2f. Although patients infected with Stx2f-producing strains usually show milder symptoms
230   (Friesema I, et al., 2014), there are a few reports of the isolation of Stx2f-producing *E. coli* from
231   HUS patients (Friesema IHM, et al., 2015; Grande L, et al., 2016), and thus the virulence potential
232   of Stx2f-producing strains has not yet been well elucidated. As expected, Stx1a was not detected
233   by the HTRF assay (Table S2).

234

Applicability of the HTRF assay to other Stx2 subtypes

235

236   Finally, we examined whether the HTRF assay can be applied to Stx2b, Stx2c, Stx2d, and

237   Stx2g, as it was to Stx2a and Stx2e. As purified preparations were not available for these four

238   subtypes, we examined them using MMC-treated STEC cell lysates, each containing Stx2b, Stx2c,

239   Stx2d, or Stx2g. For comparison, Stx2a-, Stx2e-, and Stx2f-containing cell lysates and that of an

240   *stx*-negative strain (MG1655) were also included in this analysis. Note that before this analysis,

241   we confirmed that each of the STEC strains used possessed a single *stx2* gene by BLASTN search

242   of whole genome sequences, five of which were determined in this study.

243   As shown in Table 1, the HTRF assay detected the four Stx2 subtypes in each STEC

244   lysate and provided their estimated concentrations in each lysate. No signal intensity was obtained

245   in the cell lysate of the *stx*-negative *E. coli* strain. We then measured the concentrations of the Stx2

246   subtypes using the VTEC-RPLA system with Stx2a as a standard (see methods) (Table 1) and

247   compared them with those estimated by the HTRF assay. The results indicated that the Stx

248   concentrations estimated by the two systems correlated very well (Pearson's r = 0.9989, P <

249   0.0001; Fig. 3).

250   In the comparison of amino acid sequences of mature Stx proteins (leader signal-

251   removed) with those of Stx2a, there were 3-92 amino acid substitutions in Stx2 subtypes (Fig. S1):

252   19 (14 in A-subunit + 5 in B-subunit) in Stx2b, 3 (1 + 2) in Stx2c, 4 or 5 (2 or 3 + 2) in Stx2d, 26

253   (17 + 9) in Stx2e, 92 (83 + 9) in Stx2f, and 18 (14 + 4) in Stx2g. Thus, except for Stx2f, Stx2e is

254   most dissimilar to Stx2a in amino acid sequence (92.9% identity). As already described, the HTRF

255   signals of Stx2e were nearly identical to those of Stx2a (Fig. 2). These results suggest that the two

256   mAbs used in this system recognize the epitopes common to Stx2a and Stx2e. The numbers of

257   amino acid residues in the four Stx2 subtypes (Stx2b, Stx2c, Stx2d, and Stx2g), different from

258   those shared by Stx2a and Stx2e, were less than 10 residues in the A-subunits of each subtype (10

259   in Stx2b, 1 in Stx2c, 0 or 1 in Stx2d, and 7 in Stx2g) and one residue in the B-subunits of each

260   subtype. Such a high similarity in primary structure between Stx2 subtypes except for Stx2f

261   suggests that they exhibit very similar reactivities to the two mAbs. Thus, the concentrations of

262   Stx2 subtypes estimated by the HTRF assay using Stx2a as a standard most likely represent

263   concentrations very close to the true concentrations, which could be determined by using the

264   cognate Stx subtype as a reference. The high-level correlation of the Stx concentrations estimated

265   by the HTRF assay with those estimated by the pAb-based VTEC-RPLA system shown in Fig. 3

266 gives some support to this assumption, although small structural differences between the Stx2

267 subtypes could affect the signal intensities to some extent in the assay due to the differences in

268 affinities of antibodies to antigens and/or physical distances between donors and acceptors.

269   Finally, we measured the concentrations of Stx2a, Stx2e, and Stx2g in the cell lysates

270 which were prepared without MMC treatment from strains Sakai, EC-PM083, and KS-P022,

271 respectively, using the HTRF assay we developed. While the concentrations were much lower than

272 those with MMC-treatment as expected, the concentrations of these toxins were successfully

273 determined (68.0 ± 3.9 ng/ml in Sakai, 20.6 ± 0.3 ng/ml in EC-PM083, and 5.0 ± 0.8 ng/ml in KS-

274 P022; data from three independent experiments presenting the mean value $\pm$ SD).

275

276 **Conclusion**

277   We developed the HTRF assay for quantifying several Stx2 subtypes. While this assay

278 system does not detect Stx2f, Stx2e can be quantified similarly to Stx2a, and other Stx2 subtypes

279 (Stx2b, 2c, 2d, and 2g) can also be quantified at a certain level of accuracy. The HTRF protocol is

280 simple, avoiding technical errors. In addition, this assay is not an endpoint assay like RPLA, and

281 its working range (1-64 ng/ml for Stx2a and Stx2e) is likely wide enough. Due to these advantages,

282 this assay system is applicable to the analysis of Stx2 production levels of a large number of STEC

283 strains. It should be noted, however, that although this assay may be applicable to the quantification

284 of these toxins in clinical and environmental samples, careful validations are required before

285 applying this assay system to these samples. Another limitation of this study is a lack of

286 comparison of this system with other quantitative assay systems to evaluate it more precisely due

287 to the restriction on their importation to our country.

288

289 **Acknowledgments**

290   We thank M. Horiguchi and K. Ozaki for providing technical assistance. We also thank

291 N. Ishijima and R. Tohya for providing the Stx2f toxoid and *stx2e*-positive STEC strains,

292 respectively.

293

294 **References**

295 Arimitsu H, Sasaki K, Kojima H, Yanaka T, Tsuji T. 2013a. Simple method for Shiga toxin 2e

296   purification by affinity chromatography via binding to the divinyl sulfone group. PLoS One

297   8: e83577.

298   Arimitsu H, Sasaki K, Shimizu T, Tsukamoto K, Shimizu T, Tsuji T. 2013b. Large-scale
299   preparation of Shiga toxin 2 in *Escherichia coli* for toxoid vaccine antigen production.
300   Microbiology and Immunology 57: 38–45.

301   Arimitsu H, Sasaki K, Tsuji T. 2016. Development of a simple and rapid diagnosis method for
302   swine edema disease to specifically detect Stx2e protein by immunochromatographic test.
303   Microbiology and Immunology 60: 334–342.

304   Arimizu Y, Kirino Y, Sato MP, Uno K, Sato T, Gotoh Y, Auvray F, Brugere H, Oswald E, Mainil
305   JG, Anklam KS, Döpfer D, Yoshino S, Ooka T, Tanizawa Y, Nakamura Y, Iguchi A, Morita-
306   Ishihara T, Ohnishi M, Akashi K, Hayashi T, Ogura Y. 2019. Large-scale genome analysis of
307   bovine commensal *Escherichia coli* reveals that bovine-adapted *E. coli* lineages are serving
308   as evolutionary sources of the emergence of human intestinal pathogenic strains. Genome
309   Research 29: 1495–1505.

310   Armstrong CM, Ruth LE, Capobianco JA, Strobaugh Jr TP, Rubio FM, Gehring AG. 2018.
311   Detection of Shiga toxin 2 produced by *Escherichia coli* in foods using a novel AlphaLISA.
312   Toxins 10: 422.

313   Beutin L, Zimmermann S, Gleier K. 1996. Rapid detection and isolation of Shiga-like toxin
314   (Verocytotoxin)-producing *Escherichia coli* by direct testing of individual enterohemolytic
315   colonies from washed sheep blood agar plates in the VTEC-RPLA assay. Journal of Clinical
316   Microbiology 34: 2812-2814.

317   Bielaszewska M, Mellmann A, Bletz S, Zhang W, Köck R, Kossow A, Prager R, Fruth A, Orth-
318   Höller D, Marejková M, Morabito S, Caprioli A, Piérard D, Smith G, Jenkins C, Curová K,
319   Karch H. 2013. Enterohemorrhagic *Escherichia coli* O26:H11/H-: A new virulent clone
320   emerges in Europe. Clinical Infectious Diseases 56: 1373–1381.

321   Blattner FR, Plunkett 3rd G, Bloch CA, Perna NT, Burland V, Riley M, Collado-Vides J, Glasner
322   JD, Rode CK, Mayhew GF, Gregor J, Davis NW, Kirkpatrick HA, Goeden MA, Rose DJ,
323   Mau B, Shao Y. 1997. The complete genome sequence of *Escherichia coli* K-12. Science 277:
324   1453-1462.

325   Carter MQ, Pham A, Du WX, He X. 2021. Differential induction of Shiga toxin in environmental
326   *Escherichia coli* O145:H28 strains carrying the same genotype as the outbreak strains.
327   International Journal of Food Microbiology 339: 109029.

328   Centers for Disease Control and Prevention (CDC). 2018. National enteric disease surveillance:
329   Shiga toxin-producing *Escherichia coli* (STEC) annual report, 2016 Available at
330   https://www.cdc.gov/ecoli/surv2016/index.html (accessed 31 March 2021).

331   Chart H, Willshaw GA, Cheasty T. 2001. Evaluation of a reversed passive latex agglutination test
332   for the detection of Verocytotoxin (VT) expressed by strains of VT-producing *Escherichia*
333   *coli*. Letters in Applied Microbiology 32: 370-374.

334   Cohen N, Mechaly A, Mazor O, Fisher M, Zahavy E. 2014. Rapid homogenous time-resolved
335   fluorescence (HTRF) immunoassay for anthrax detection. Journal of Fluorescence 24: 795-
336   801.

337   Dallman TJ, Ashton PM, Byrne L, Perry NT, Petrovska L, Ellis R, Allison L, Hanson M, Holmes
338   A, Gunn GJ, Chase-Topping ME, Woolhouse ME, Grant KA, Gally DL, Wain J, Jenkins C.
339   2015. Applying phylogenomics to understand the emergence of Shiga-toxin-producing
340   *Escherichia coli* O157:H7 strains causing severe human disease in the UK. Microbial
341   Genomics 1: e000029.

342   Degorce F, Card A, Soh S, Trinquet E, Knapik GP, Xie B. 2009. HTRF: A technology tailored for
343   drug discovery - a review of theoretical aspects and recent applications. Current Chemical
344   Genomics 3: 22–32.

345   European Food Safety Authority and European Centre for Disease Prevention and Control (EFSA
346   and ECDC). 2019. The European union one health 2018 zoonoses report. EFSA Journal. 17:
347   e05926.

348   Fuller CA, Pellino CA, Flagler MJ, Strasser JE, Weiss AA. 2011 Shiga toxin subtypes display
349   dramatic differences in potency. Infection and Immunity 79: 1329–1337.

350   Friesema IHM, Keijzer-Veen MG, Koppejan M, Schipper HS, van Griethuysen AJ, Heck MEOC,
351   van Pelt W. 2015 Hemolytic uremic syndrome associated with *Escherichia coli* O8:H19 and
352   Shiga toxin 2f gene. Emerging Infectious Disease 21: 168-169.

353   Friesema I, van der Zwaluw K, Schuurman T, Kooistra-Smid M, Franz E, van Duynhoven Y, van
354   Pelt W. 2014 Emergence of Escherichia coli encoding Shiga toxin 2f in human Shiga toxin-
355   producing E. coli (STEC) infections in the Netherlands, January 2008 to December 2001.
356   Eurosurveillance 19: 26-32.

357   Grande L, Michelacci V, Bondì R, Gigliucci F, Franz E, Badouei MA, Schlager S, Minelli F,
358   Tozzoli R, Caprioli A, Morabito S. 2016 Whole-genome characterization and strain

359   comparison of VT2f-producing *Escherichia coli* causing hemolytic uremic syndrome.
360   Emerging Infectious Disease 22: 2078-2086.

361 Hayashi T, Makino K, Ohnishi M, Kurokawa K, Ishii K, Yokoyama K, Han CG, Ohtsubo E,
362   Nakayama K, Murata T, Tanaka M, Tobe T, Iida T, Takami H, Honda T, Sasakawa C,
363   Ogasawara N, Yasunaga T, Kuhara S, Shiba T, Hattori M, Shinagawa H. 2001. Complete
364   genome sequence of enterohemorrhagic *Eschelichia coli* O157:H7 and genomic comparison
365   with a laboratory strain K-12. DNA Research 8: 11–22.

366 He X, Ardissino G, Patfield S, Cheng LW, Silva CJ, Brigotti M. 2018. An improved method for
367   the sensitive detection of Shiga toxin 2 in human serum. Toxins 10: 59.

368 Ishijima N, Lee K, Kuwahara T, Nakayama-Imaohji H, Yoneda S, Iguchi A, Ogura Y, Hayashi T,
369   Ohnishi M, Iyoda S. 2017. Identification of a new virulent clade in enterohemorrhagic
370   *Escherichia coli* O26:H11/H- sequence type 29. Scientific Reports 7: 43136.

371 Joensen KG, Tetzschner AM, Iguchi A, Aarestrup FM, Scheutz F. 2015. Rapid and easy *in silico*
372   serotyping of *Escherichia coli* isolates by use of whole-genome sequencing data. Journal of
373   Clinical Microbiology 53: 2410–2426.

374 Karmali MA, Petric M, Bielaszewska M. 1999. Evaluation of a microplate latex agglutination
375   method (Verotox-F assay) for detecting and characterizing Verotoxins (Shiga toxins) in
376   *Escherichia coli*. Journal of Clinical Microbiology 37: 396-399.

377 Nakamura K, Murase K, Sato MP, Toyoda A, Itoh T, Mainil JG, Piérard D, Yoshino S, Kimata K,
378   Isobe J, Seto K, Etoh Y, Narimatsu H, Saito S, Yatsuyanagi J, Lee K, Iyoda S, Ohnishi M,
379   Ooka T, Gotoh Y, Ogura Y, Hayashi T. 2020. Differential dynamics and impacts of prophages
380   and plasmids on the pangenome and virulence factor repertoires of Shiga toxin-producing
381   *Escherichia coli* O145:H28. Microbial Genomics 6: e000323.

382 National Institute of Infectious Diseases (NIID). 2018. Enterohemorrhagic *Escherichia coli*
383   (EHEC) infection, as of March 2018, Japan. Infectious Agents Surveillance Report 39: 71–
384   72.

385 Ogura Y, Mondal SI, Islam MR, Mako T, Arisawa K, Katsura K, Ooka T, Gotoh Y, Murase K,
386   Ohnishi M, Hayashi T. 2015. The Shiga toxin 2 production level in enterohemorrhagic
387   *Escherichia coli* O157:H7 is correlated with the subtypes of toxin-encoding phage. Scientific
388   Reports 5: 16663.

389 Ogura Y, Seto K, Morimoto Y, Nakamura K, Sato MP, Gotoh Y, Itoh T, Toyoda A, Ohnishi M,

390   Hayashi T. 2018. Genomic characterization of β-glucuronidase-positive *Escherichia coli*
391   O157:H7 producing Stx2a. Emerging Infectious Diseases 24: 2219–2227.

392   Parsons BD, Zelyas N, Berenger BM, Chui L. 2016. Detection, characterization, and typing of
393   Shiga toxin-producing *Escherichia coli*. Frontiers in Microbiology 7: 478.

394   Quiñones B, Massey S, Friedman M, Swimley MS, Teter K. 2009. Novel cell-based method to
395   detect Shiga toxin 2 from *Escherichia coli* O157:H7 and inhibitors of toxin activity. Applied
396   and Environmental Microbiology 75: 1410–1416.

397   Rahman M, Nabi A, Asadulghani Md, Faruque SM, Islam MA. 2018 Toxigenic properties and stx
398   phage characterization of *Escherichia coli* O157 isolated from animal sources in a developing
399   country setting. BMC Microbiology 18: 98.

400   Scheutz F, Teel LD, Beutin L, Piérard D, Buvens G, Karch H, Mellmann A, Caprioli A, Tozzoli
401   R, Morabito S, Strockbine NA, Melton-Celsa AR, Sanchez M, Persson S, O'Brien AD. 2012.
402   Multicenter evaluation of a sequence-based protocol for subtyping Shiga toxins and
403   standardizing Stx nomenclature. Journal of Clinical Microbiology 50: 2951–2963.

404   Skinner C, Patfield S, Stanker L, He X. 2013. Development of monoclonal antibodies and
405   immunoassays for sensitive and specific detection of Shiga toxin Stx2f. PLoS One 8: e76563.

406   Smith AM, Tau NP, Kalule BJ, Nicol MP, McCulloch M, Jacobs CA, McCarthy KM, Ismail A,
407   Allam M, Kleynhans J. 2019. Shiga toxin-producing *Escherichia coli* O26:H11 associated
408   with a cluster of haemolytic uraemic syndrome cases in South Africa, 2017. Access
409   Microbiology 1: e000061.

410   Yamasaki E, Watahiki M, Isobe J, Sata T, Nair GB, Kurazono H. 2015. Quantitative detection of
411   Shiga toxins directly from stool specimens of patients associated with an outbreak of
412   enterohemorrhagic Escherichia coli in Japan–quantitative Shiga toxin detection from stool
413   during EHEC outbreak. Toxins 7: 4381–4389.

414   Yamazaki M, Sato S, Gondaira F, Sugiyama J. 2013. A rapid bioluminescent enzyme
415   immunoassay (BLEIA) for the detection of Shiga toxin types 1 and 2. Microbiology and
416   Immunology. 45: 621–628.

Figure 1

Optimization of the HTRF assay for Stx2 detection.

The HTRF assay conditions were optimized by selecting the most suitable antibody pair and incubation time (A) and determining the most appropriate concentrations of antibodies (B). The relative amount of Stx toxin (commercially available lyophilized Stx2; see Methods) used in each assay is presented as the reciprocal of the final dilution factor on the X-axis. Delta F (DF) values were used as the signal intensities of each reaction. All data are presented as the mean values (n=3).

A

Donor (Eu)/Acceptor (d2)
LS-C132889/20273-04

20273-04/LS-C132889

MBS313194/20273-04

20273-04/MBS313194

MBS313194/LS-C132889

LS-C132889/MBS313194

incubation time (hr)
0.5   1   2   4   8   18

B

d2-labbeld Ab: 1.0 µg/ml

Eu-labbeld Ab: 0.5 µg/ml

Eu-labbeld Ab (µg/ml)
0.06   0.13
0.25   0.5

d2-labbeld Ab (µg/ml)
0.4   0.8
1.6   3.2
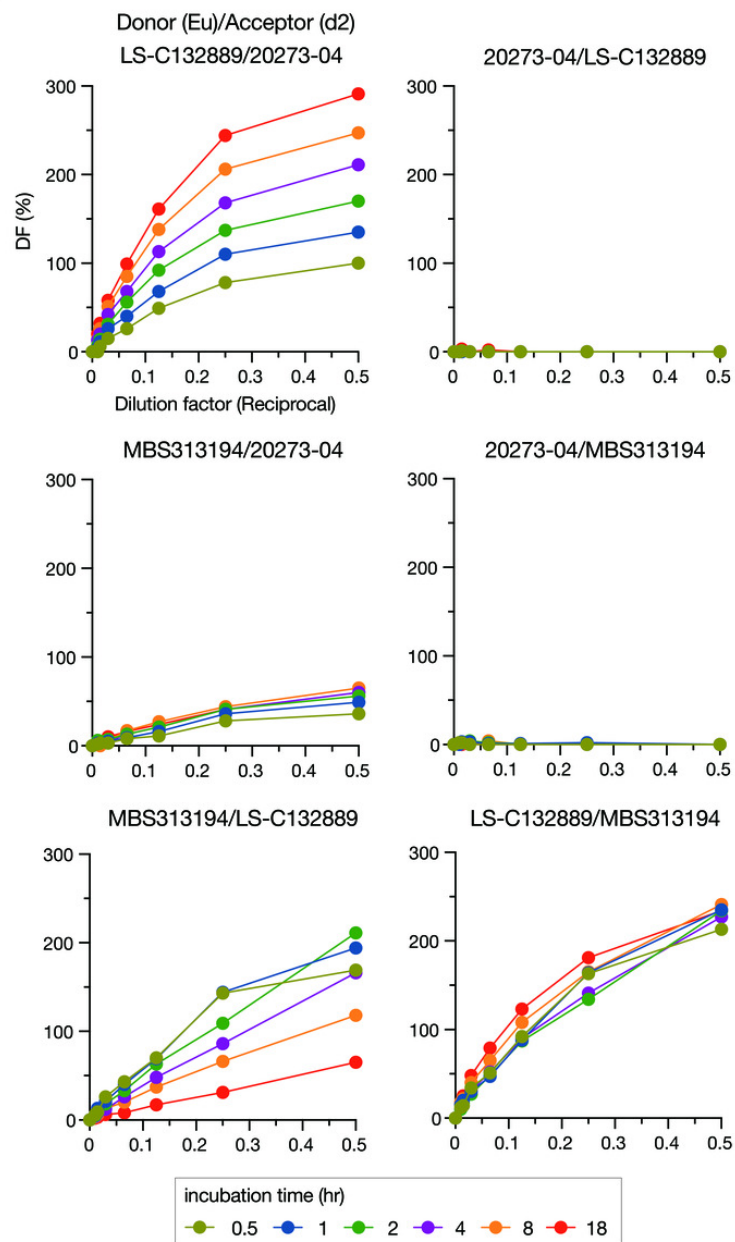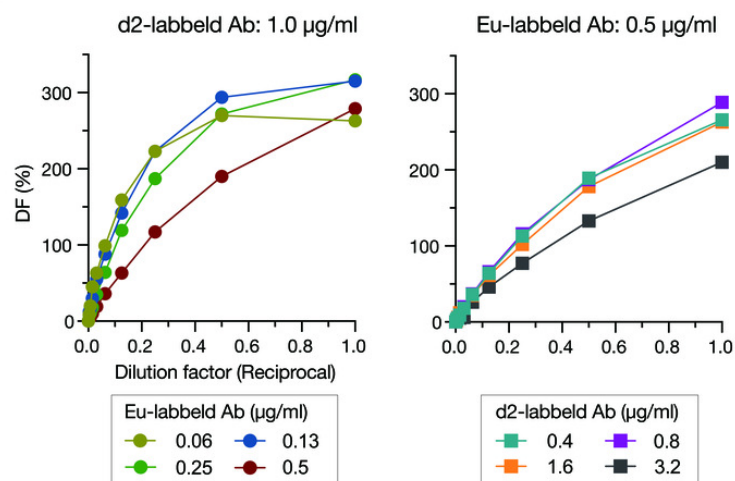
Figure 2

Dynamic ranges of the HTRF assay for purified Stx2a and Stx2e.

In the left panels, delta ratio (DR) values at each Stx2 concentration ranging from 1 ng/ml to 256 ng/ml are shown. All measurements were conducted in triplicate, and data are presented as the mean values ± standard deviation. In the right panels, DR values at Stx2 concentrations ranging from 1 ng/ml to 64 ng/ml in a representative assay are shown. A weighted four parameter logistic (4PL) curve can be applied to the analysis of the DRs in this range of Stx2 concentrations.
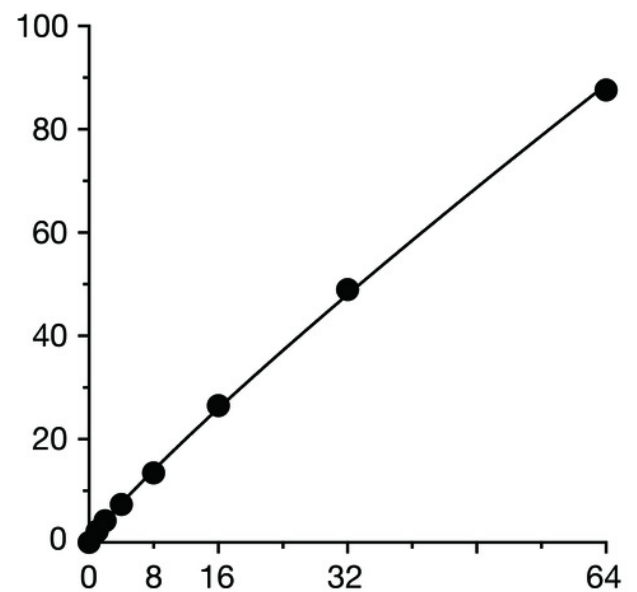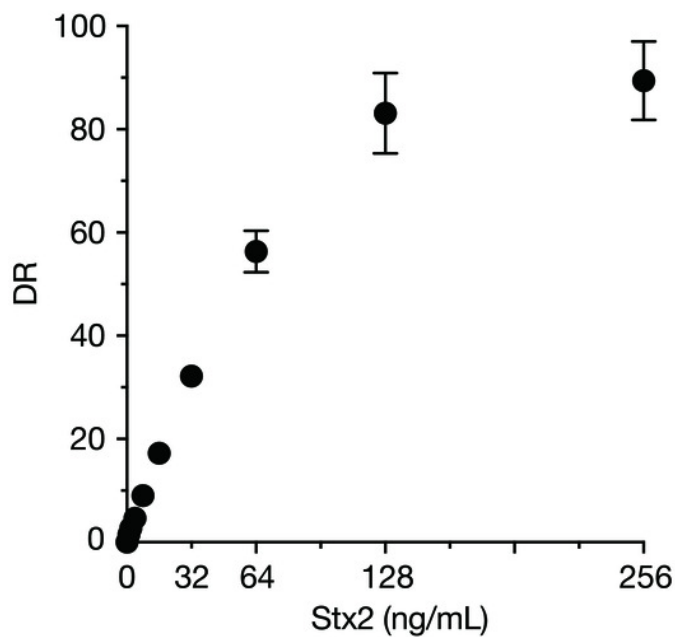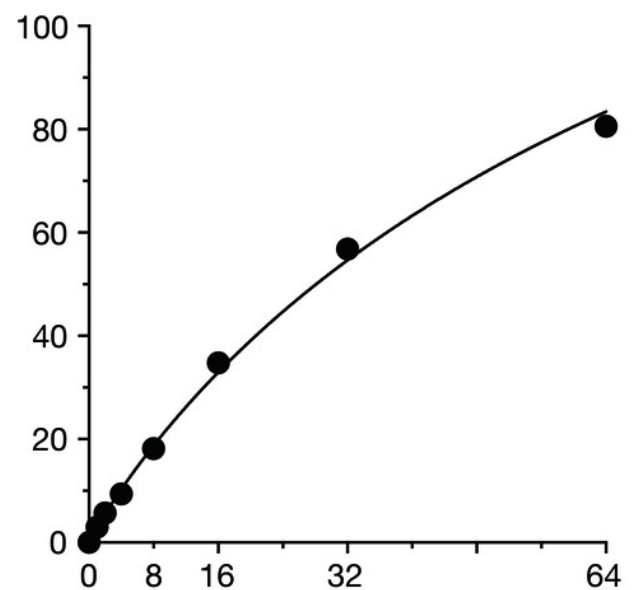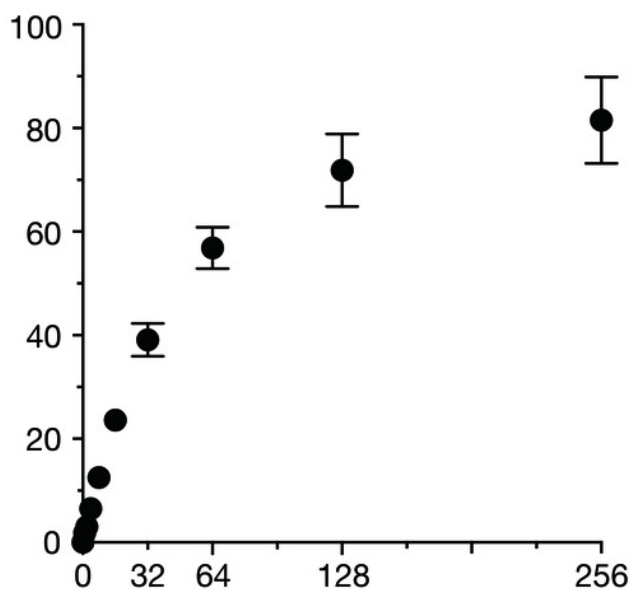
Figure 3

Relationship between the Stx2 concentrations estimated by the HTRF and RPLA assays.

The concentration of Stx2 produced by each STEC strain (shown in parentheses) was measured by HTRF and RPLA assays. Each plot represents the mean values of Stx2 concentrations determined by three independent HTRF assays (X-axis) and the RPLA unit obtained from a single assay (Y-axis). Each value is shown in Table 1. See Methods for the definition of units in the RPLA assay. Note that rabbit anti-Stx2 pAb was used in the RPLA assay. Both axes are displayed in logarithmic scale. The solid line represents the nonlinear regression. The correlation between the data from the two assay systems was evaluated using the Pearson correlation coefficient, as shown in the graph.
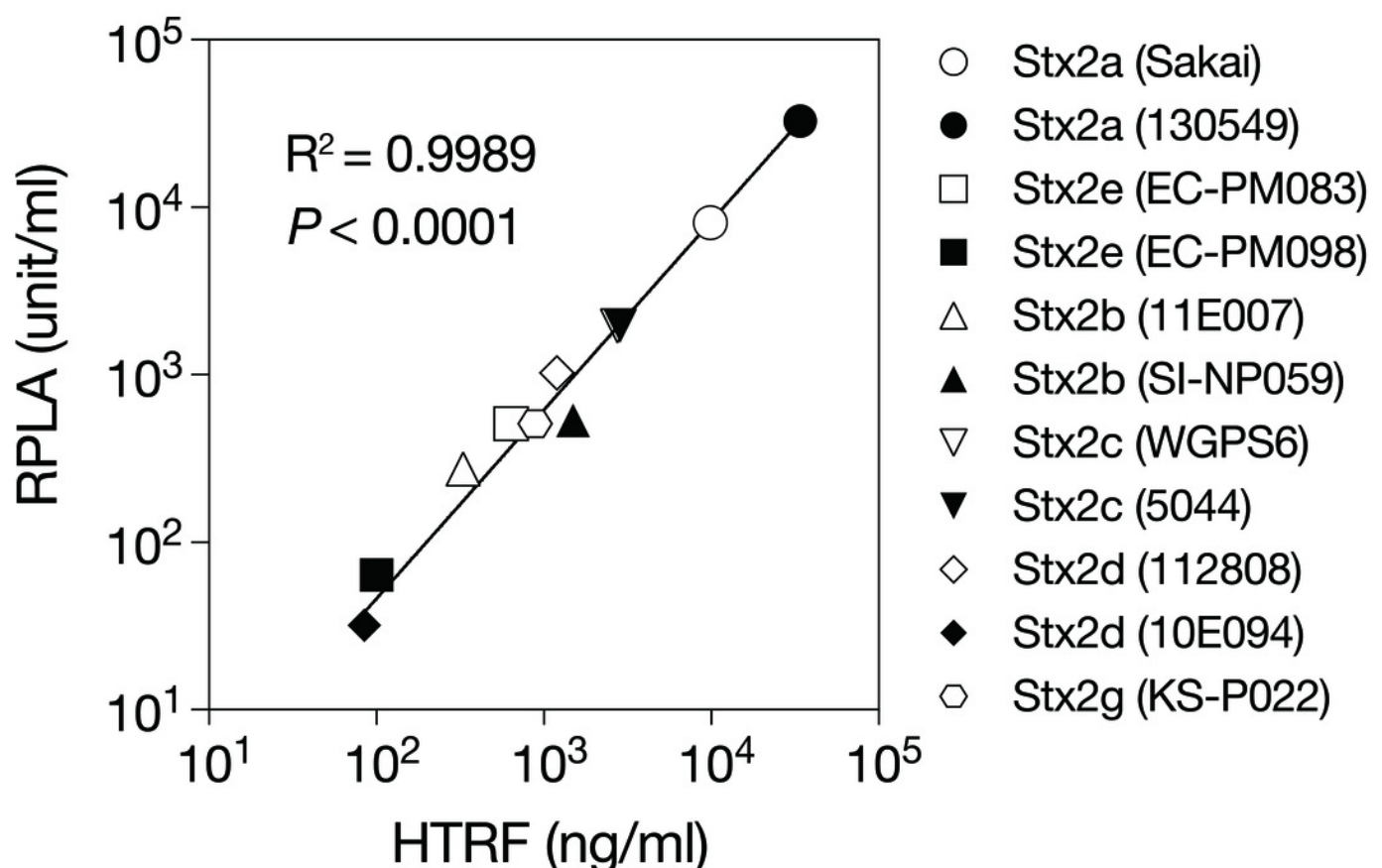
STEC strains used in this study and their Stx2 production levels determined by HTRF and RPLA assay.

Table 1. STEC strains used in this study and their Stx2 production levels determined by HTRF and RPLA assay

| Strain | Serotype | Source | *stx* subtype | Stx2 titer | | Accession No. | Reference |
				HTRF (ng/ml)[*]	RPLA (unit/ml)[†]		
Sakai	O157:H7	Human	*stx1a*/*stx2a*	9,900±520	8,092	BA000007	Hayashi, et al. 2001.
130549	O26:H11	Human	*stx2a*	34,000±1,500	32,768	BDHP01000185	Ishijima, et al. 2017.
11E007	O146:H21	Human	*stx2b*	330±39	256	BOUS01000033	This study
SI-NP059	Onovel1:H16	Bovine	*stx2b*	1,500±120	512	BGIA01000167	Arimizu, et al. 2019.
WGPS6	O157:H7	Human	*stx2c*	2,700±79	2,048	AP012539	Ogura, et al. 2015.
5044	O145:H28	Human	*stx2c*	2,800±160	2,048	BJPC01000106	Nakamura, et al. 2020.
112808	O145:H28	Human	*stx1a*/*stx2d*	1,200±400	1,024	BJQB01000217	Nakamura, et al. 2020.
10E094	OUT:H7	Human	*stx2d*	85±5	32	BOUT01000015	This study
EC-PM083	O157:H19	Swine	*stx2e*	640±90	512	BOUQ01000003	This study
EC-PM098	O50:H32 or O2:H32	Swine	*stx2e*	100±20	64	BOUR01000009	This study
07E033	O63:H6	Human	*stx2f*	N.D.	128	BOUS01000033	This study
KS-P022	O168:H8	Bovine	*stx2g*	890±170	512	BGAG01000027	Arimizu, et al. 2019.
MG1655	O16:H48	Widely used laboratory strain	*stx-*negative	N.D.	N.D.	U00096	Blattner, et al. 1997.

UT, untypable

N.D., not detected

[*] Technical triplicate (mean value ± SD)

[†] 1 unit/ml roughly corresponds to 1 ng/ml of Stx2a (see Methods)